



HAL
open science

Structure of Au on Ag(110) studied by scanning tunneling microscopy

S Chiang, S Rousset, De Fowler, Dd Chambliss

► **To cite this version:**

S Chiang, S Rousset, De Fowler, Dd Chambliss. Structure of Au on Ag(110) studied by scanning tunneling microscopy. *Journal of Vacuum Science & Technology B Microelectronics and Nanometer Structures*, 1994, 12 (3), pp.1747-1750. 10.1116/1.587590 . hal-01987623

HAL Id: hal-01987623

<https://hal.science/hal-01987623>

Submitted on 10 Apr 2020

HAL is a multi-disciplinary open access archive for the deposit and dissemination of scientific research documents, whether they are published or not. The documents may come from teaching and research institutions in France or abroad, or from public or private research centers.

L'archive ouverte pluridisciplinaire **HAL**, est destinée au dépôt et à la diffusion de documents scientifiques de niveau recherche, publiés ou non, émanant des établissements d'enseignement et de recherche français ou étrangers, des laboratoires publics ou privés.



Distributed under a Creative Commons Attribution 4.0 International License

Structure of Au on Ag(110) studied by scanning tunneling microscopy

S. Chiang, S. Rousset,^{a)} D. E. Fowler, and D. D. Chambliss
IBM Research Division, Almaden Research Center, San Jose, California 95120-6099

(Received 9 August 1993; accepted 5 January 1994)

The epitaxial growth of Au on Ag(110) has been studied by scanning tunneling microscopy up to 8 ML. In the submonolayer range the results show that gold atoms are intermixed with the silver atoms in the top two layers. Above 1 ML a two-dimensional fingerlike growth gives rise to anisotropic three-dimensional islands of gold, which appear to be thermal equilibrium structures. Above 5 ML, the gold overlayer forms a (1×3) reconstruction which is manifested as double rows of atoms growing along $[1\bar{1}0]$. The development of this reconstruction is followed as a function of coverage.

I. INTRODUCTION

The field of epitaxial growth of metal overlayers on metal substrates has been of great interest for many years. The classification of epitaxial growth into three general growth modes has been given in terms of the relative surface free energies of the different metals.¹ For the system of Au on Ag(110), because of the extremely close lattice parameters ($a_{\text{Au}}=4.08 \text{ \AA}$, $a_{\text{Ag}}=4.09 \text{ \AA}$) and surface free energies, simple layer-by-layer growth would have been expected. Recently, however, it has been found that a unique growth mode occurs which has been described as "intermixed Stranski-Krastanov" growth,² in contrast to earlier reports of bilayer growth for this system.^{3,4} This description is supported by both experiments^{2,5} and first principles theoretical calculations.^{6,7} Up to ~ 1 ML, most of the incoming Au goes underneath the top layer of Ag. For higher coverage, the Au appears to grow on top of the intermixed layer, first as two-dimensional (2D) fingers from step edges, and then as three-dimensional (3D) anisotropic islands. The scanning tunneling microscope (STM) has proven to be an extremely useful tool for exploring this system.

In this article, we briefly summarize our earlier STM results for Au on Ag(110) at low coverage ($\theta < 2$ ML).^{2,5} We present new data for this system suggesting that the 3D islands are indeed thermal equilibrium structures; then we describe samples with higher coverages of Au ($2 \text{ ML} < \theta < 8$ ML). The Au continues to grow in an anisotropic fashion along the $[1\bar{1}0]$ direction of the underlying Ag(110) substrate. Long rows of atoms grow along $[1\bar{1}0]$ and eventually form the Au (1×3) reconstruction. We follow the development of this reconstruction as a function of Au coverage through our STM images.

II. EXPERIMENT

The multichamber ultrahigh vacuum STM apparatus has been described in detail elsewhere.⁸ The Ag(110) crystal was cleaned by Ar-ion bombardment (500 eV) and flash annealed at 600 °C. After the sample was allowed to cool for at least 1 h to reach room temperature (RT), it was exposed to Au flux evaporated from a W basket. Au flux was measured using a

line-of-sight ionization gauge. For coverages up to 2 ML, most of the evaporations were performed at a constant rate of 0.6 ML/min ($1 \text{ ML}_{\text{Ag(110)}}=8.45 \times 10^{14} \text{ atoms/cm}^2$), and the gauge was calibrated for Au within 20% by optimizing the sharp $c(2 \times 2)$ low energy electron diffraction (LEED) pattern obtained when $0.5 \text{ ML} \pm 0.1 \text{ ML}$ of Au is deposited onto Cu(100).⁹ For coverages from 2 to 8 ML, the deposition rate was ~ 3.5 ML/min, and the coverage is only accurate to ± 0.5 ML. Following sample preparation, no contamination of the surface with O or C was found by Auger spectroscopy. For coverages up to ~ 4 ML, the observed LEED pattern was (1×1). At ~ 5.5 ML, some faint streaks along (1×3) spot positions appeared. For higher coverage, (1×3) LEED patterns were observed with some broadening of spots. The STM experiments were usually performed within a few hours after deposition. All STM images were acquired in constant current mode. Low coverage samples (< 2 ML) were mainly measured with negative sample voltage from 30 mV to 2 V, and high coverage samples ($2 \text{ ML} < \theta < 8$ ML) were mostly measured with positive sample voltage from 0.1 to 1 V; tunneling currents were generally from 1 to 2 nA. Reversing the sample polarity did not show any spectroscopic effects. Each image was recorded in ~ 5 –10 min. Linear or quadratic background planes have been subtracted from the images, and images were corrected for thermal drift.

III. RESULTS AND DISCUSSION

Au on Ag(110) has previously been studied for coverages from 0.05 to 15 ML by medium energy ion scattering (MEIS) by Fenter and Gustafsson.^{3,4} They interpreted their low coverage blocking curves, however, as evidence for bilayer growth for $\theta > 0.06$ ML. At higher coverage ($4 \text{ ML} < \theta < 7$ ML), they report a (1×3) reconstruction of Au. At even higher coverage ($8 \text{ ML} < \theta < 15$ ML), they finally observed the (1×2) reconstruction which is characteristic of clean Au(110). The energetics of fcc(110) missing row reconstructions have been previously calculated for pure metals.¹⁰

The system has also recently been studied by synchrotron core-level photoemission and reflection high-energy electron diffraction (RHEED) by Hirschorn *et al.*¹¹ Although they agree that Au and Ag interchange for $\theta < 1$ ML, they believe that this exchange process continues for multilayer cover-

^{a)}Permanent address: Groupe de Physique des Solides, CNRS—Universités de Paris VI et VII, Tour 23, 2 Place Jussieu, 75251 Paris Cedex 05, France.

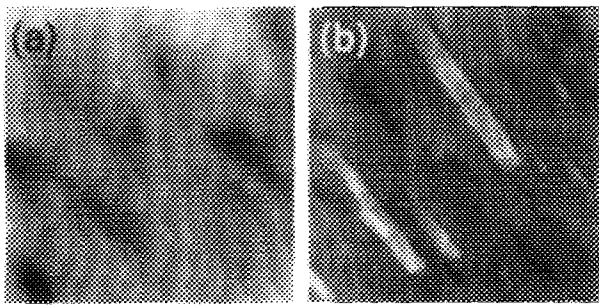


FIG. 1. STM top view images. (a) 1.0 ML Au on Ag(110), with 2D finger growth from monoatomic steps, $\sim 900 \text{ \AA} \times 900 \text{ \AA}$. (b) STM top view image for 1.4 ML Au on Ag(110) shows transition in growth from 2D fingers to 3D islands, $1500 \text{ \AA} \times 1500 \text{ \AA}$.

ages. In fact, they suggest that $(1 - \delta)^N$ is the surface area still covered by Ag after growth of N monolayers, with $\delta = 0.11$. In addition, their RHEED studies saw (1×2) reconstruction beginning at coverages as low as 0.5 ML, and continuing up to 100 ML. They saw no sign of a (1×3) reconstruction at intermediate coverages, which was reported in the earlier MEIS study⁴ and is also observed in the present work. Thus it appears that there must have been some differences in the sample preparation in Hirschorn *et al.*'s work, perhaps related to substrate cleanliness or ordering, compared with the other studies of Au on Ag(110).

A. Intermixing growth

The STM images of Au on Ag(110) show no islands and no evidence for bilayer steps for $\theta < 1$ ML. Figure 1(a) shows a STM image for $\theta \approx 1$ ML with single height atomic steps only. If there are no bilayer steps, we must seek another explanation of the MEIS blocking curves, which indicate that Au atoms are shadowed even at coverages as low as 0.06 ML.^{3,4} A possible explanation is intermixing of the incoming Au with the Ag substrate atoms. We quantitatively reinterpreted the MEIS blocking curves by using standard Monte Carlo-type scattering calculations¹² to determine the fractions of the surface covered by three possible Au/Ag configurations: (1) Au on top of the Ag(110) surface, (2) a variable quantity of Au incorporated below the top layer of the Ag(110) surface, and (3) Au bilayers on top of the Ag(110) surface. The details of the calculations are given elsewhere.² The results of our modeling give a best-fit to the blocking curve data when nearly all of the Au atoms are located below the top Ag layer. For submonolayer coverage of Au, the combination of STM and MEIS data gives a consistent picture, where deposited Au atoms are incorporated mainly in the second layer [see, Figs. 2(a)–2(b)].

Recent first principles total energy calculations showed first, that Au bilayers were unlikely to occur in thermal equilibrium.⁶ Subsequent calculations showed that the most favorable initial growth process up to 1 ML Au would proceed via subsurface substitution,⁷ agreeing with our conclusion based on the experimental data. This suggests that our observations for $\theta < 1$ ML are likely to reflect the equilibrium growth mode of the system, rather than a kinetically limited process.

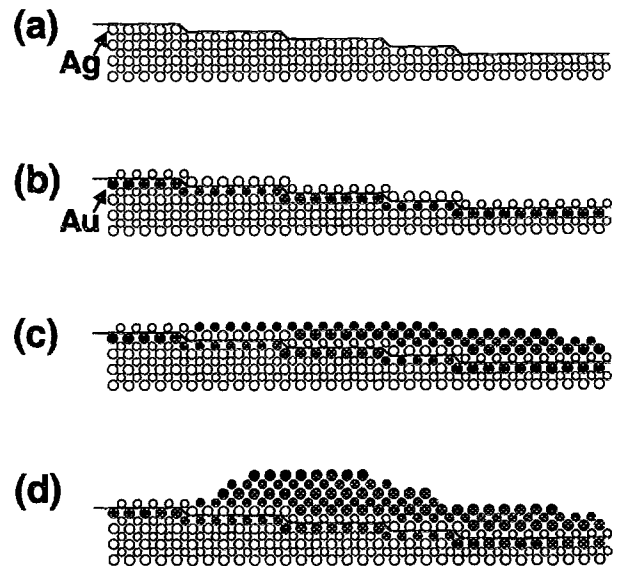


FIG. 2. Schematic diagram showing stages of "intermixed Stranski-Krastanov" growth mode for Au/Ag(110). Filled (open) circles indicate Au (Ag) atoms. Two circle sizes denote atoms in different vertical (001) planes. (a) Clean Ag(110), with line showing initial step positions. For clarity, steps are drawn more closely spaced than in actual sample. (b) ~ 1 ML Au on Ag(110), with nearly all Au atoms underneath top layer of Ag atoms. (c) 2D finger growth of Au on top of intermixed layer. (d) Further growth leads to 3D islands forming on top of intermixed layer.

B. Growth of 3D islands

For Au coverage of 1.4 ML, we had previously observed 2-D finger growth from step edges [Fig. 1(b)], developing into widely spaced, anisotropic 3D islands at coverages of ~ 2 – 3 ML.² Figures 2(c)–2(d) show a schematic diagram of these stages of growth. The data presented in this article suggest that the extent of this 3D growth is sensitive to temperature and time delay between deposition and measurement. A shortened cooling time of 30 min (versus our customary 60 min) after the final anneal may have resulted in a substrate warmer than RT, and thus a more fully equilibrated morphology, for some results in Ref. 2. Note that our previous MEIS modeling suggested that, for $\theta > 1$ ML, layers of Au subsequently grow on top of the initial Ag/Au intermixed layer.²

Now we present additional data on the growth of 3D islands for ~ 2 ML Au on Ag(110). In Fig. 3(a), we show a deposit made at room temperature. Here 2D fingerlike growth from step edges can be seen. Some isolated islands on the finger growth can also be observed. Also apparent are some "holes" as the fingerlike growth does not completely fill in the lower layer before upper layers begin to grow. The same sample is shown on the same scale in Fig. 3(b) in an image obtained after the sample had been left for ~ 3 days in the STM ultrahigh vacuum system (base pressure $< 10^{-10}$ Torr). Anisotropic 3D islands, with typical lengths of 500–1000 \AA , separated by 500–800 \AA , are now very evident. The long axis of the islands is along the $[1\bar{1}0]$ direction of the Ag(110) substrate. Figure 3(c) shows a smaller image on the same sample, showing the multilayer, fingerlike end of two islands. Some motion of step edges at the ends of such fingers was observed in subsequent images about 10 min apart;

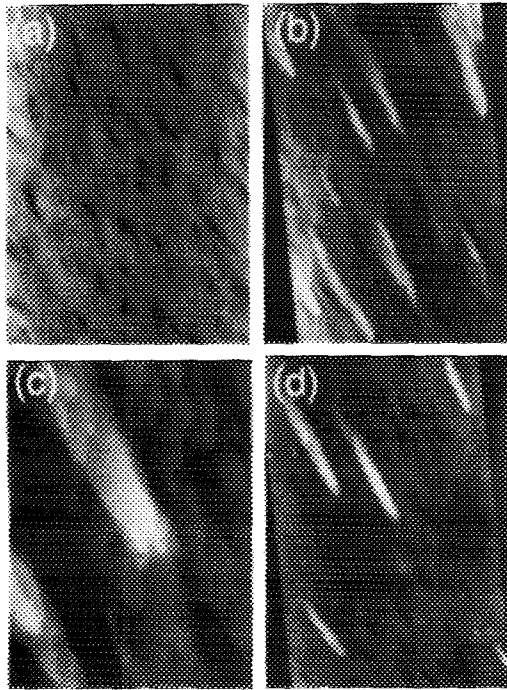


FIG. 3. (a) ~ 2 ML Au on Ag(110), deposited at room temperature, $\sim 2000 \text{ \AA} \times 3000 \text{ \AA}$. Significant growth from step edges with 3D islands beginning to form. (b) Same sample measured after three days in ultrahigh vacuum, showing significant 3D island growth along $[1\bar{1}0]$, $\sim 2000 \text{ \AA} \times 3000 \text{ \AA}$, (c) A smaller image of sample shown in (b), $\sim 650 \text{ \AA} \times 900 \text{ \AA}$, with fingerlike ends of two islands. Some atomic motion at the ends of such fingers was observed in images separated by 10 min. (d) Growth of 3D islands for ~ 2 ML Au on Ag(110) is apparently enhanced by briefly annealing sample to $\sim 80 \pm 20 \text{ }^\circ\text{C}$ after RT deposition of Au, $\sim 2000 \text{ \AA} \times 3000 \text{ \AA}$.

such step motion has frequently been observed on clean Au(110), though often on a somewhat longer time scale.¹³ These images suggest that the surface evolves with time towards the more stable 3D island structures, although surface contamination after three days is also possible. Figure 3(d), however, shows very similar 3D islands on the same scale as Fig. 3(b) and was obtained from a different sample of ~ 2 ML Au on Ag(110), with Au deposited at room temperature, and then annealed for ~ 10 min at $\sim 80 \pm 20 \text{ }^\circ\text{C}$. This implies that the 3D islands are indeed thermal equilibrium structures, as asserted above, rather than being nucleated by contamination.

C. Development of (1×3) Au reconstruction

At ~ 4 ML Au coverage, the observed LEED pattern is still (1×1) , and the STM images primarily show very flat epitaxial growth (Fig. 4). Anisotropic growth along $[1\bar{1}0]$ is still evident, with some isolated atomic-scale rows of the (1×3) structure beginning to be evident as fingerlike growth away from the deposit [Fig. 4(a)]. In addition, careful study of Fig. 4(b) indicates that most atomic rows observed are commensurate with the (1×1) structure of the (110) substrate, with several sets of isolated double rows of atoms on top of the deposit.

At higher Au coverage of ~ 5.4 – 8 ML, the (1×3) reconstruction is very evident in the STM images (Fig. 5). Clearly,

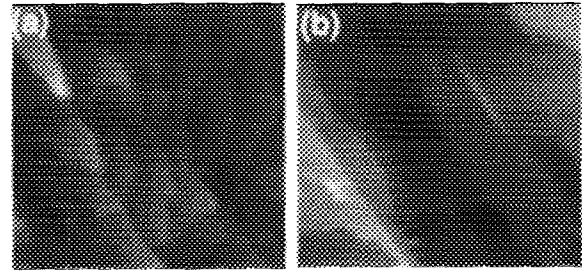


FIG. 4. ~ 4 ML Au on Ag(110), deposited at RT, showing obvious anisotropic growth along $[1\bar{1}0]$. (a) $\sim 650 \text{ \AA} \times 650 \text{ \AA}$. Note isolated rows of atoms, both growing as fingers away from deposit and on top of it. (b) $\sim 190 \text{ \AA} \times 190 \text{ \AA}$. Atomic rows commensurate with (110) substrate are evident, with several sets of isolated double rows of atoms on top of epitaxial growth.

the atomic rows of the reconstruction grow preferentially along one particular direction, which is the $[1\bar{1}0]$ direction of the substrate. From their width, the atomic rows evident in Fig. 5(c) are double rows of atoms. Thus, the (1×3) reconstruction manifests itself as double rows of atoms growing along $[1\bar{1}0]$ (see the schematic diagram in Fig. 6); such a model had been previously suggested but not experimentally confirmed.⁴ This structure is a mixture of the (1×2) missing row and (1×1) unit cells, with small (111) facets. Much disorder on an atomic scale is still apparent, with many steps, kinks, and partial rows of atoms [see Fig. 5(c)]. At ~ 8 ML, additional Au begins to form flatter epitaxial islands [Fig. 5(d)]; presumably, such structures would lead to larger terraces of (1×2) reconstructed Au at even higher coverage.

IV. CONCLUSIONS

The epitaxial growth of Au on Ag(110) is thus a very complicated system, with distinct stages of growth. By combining STM results with reexamination of the MEIS data,^{3,4}

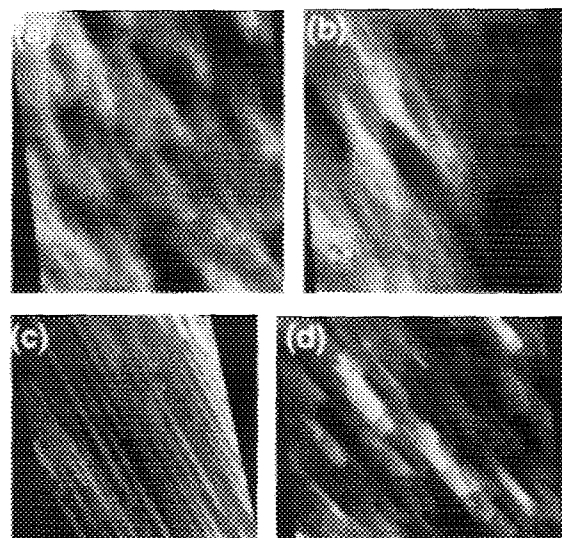


FIG. 5. Anisotropic growth along $[1\bar{1}0]$ for ~ 5.4 – 8 ML Au on Ag(110), deposited at RT. Atomic rows of (1×3) reconstruction are seen in all parts of this figure. (a) ~ 5.4 ML, $\sim 570 \text{ \AA} \times 630 \text{ \AA}$. (b) ~ 7 ML, $\sim 580 \text{ \AA} \times 680 \text{ \AA}$. (c) ~ 7 ML, $\sim 190 \text{ \AA} \times 220 \text{ \AA}$. (d) ~ 8 ML, $\sim 570 \text{ \AA} \times 550 \text{ \AA}$.

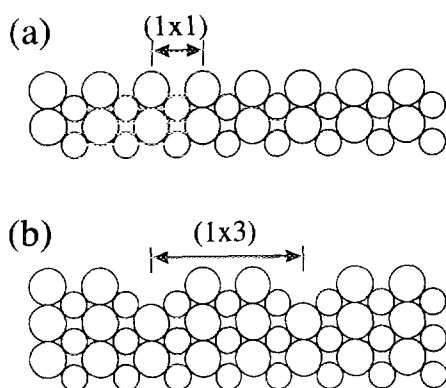


FIG. 6. Schematic diagram showing cross sections through (110) surface along [001] direction. Two circle sizes denote atoms in different vertical (001) planes. (a) (1×1) structure of unreconstructed surface. (b) Au (1×3) reconstruction model confirmed by this article, with double rows of atoms in each unit cell.

we have found that Au on Ag(110) at RT grows in an “intermixed Stranski–Krastanov” mode, starting with a Ag/Au intermixed layer followed by growth of 3D Au islands² (Fig. 2). As the 3D islands appear to be characteristic of thermal equilibrium structures, the data presented here suggest that the intermixed Stranski–Krastanov growth mode is indeed the thermal equilibrium growth. At higher coverages, we have observed very anisotropic growth along the [110] direction, leading finally to the (1×3) reconstruction of Au for $\theta \sim 6\text{--}8$ ML. Some simple simulations of the growth indicate that anisotropic sticking coefficients, with stronger sticking to rows aligned in one direction than to rows in the perpendicular direction, are more important than anisotropic diffusion effects in causing such growth.¹⁴ The anisotropic growth of the Au on Ag(110) for $\theta > 1$ ML, first in 2D fingers, then in

3D islands, and finally in the rows of the (1×3) reconstruction, is always along the [110] direction. The growth of Au on Ag(110) appears to be dominated by the effects of the rectangular substrate lattice for all coverages studied here. Far from being the simple system of layer-by-layer growth initially expected, this system has shown many interesting phenomena in its epitaxial growth.

ACKNOWLEDGMENTS

The authors would like to acknowledge M. Altman for help in cleaning the Ag(110) crystal, C. T. Chan and K.-M. Ho for sending preprints of Refs. 6 and 7, T.-C. Chiang for sending a preprint of Ref. 11, and D. Brodbeck and K. Kalki for help in image processing. This work was partially supported by the Office of Naval Research (N00014-89-C-0099).

¹E. Bauer, Z. Kristallogr. **110**, 372 (1958); Appl. Surf. Sci. **11/12**, 479 (1982).

²S. Rousset, S. Chiang, D. E. Fowler, and D. D. Chambliss, Phys. Rev. Lett. **69**, 3200 (1992).

³P. Fenter and T. Gustafsson, Phys. Rev. Lett. **64**, 1142 (1990).

⁴P. Fenter and T. Gustafsson, Phys. Rev. B **43**, 12195 (1991).

⁵S. Rousset, S. Chiang, D. E. Fowler, and D. D. Chambliss, Surf. Sci. **287**, 941 (1993).

⁶K.-P. Bohnen, C. T. Chan, and K. M. Ho, Surf. Sci. Lett. **268**, L284 (1992).

⁷C. T. Chan, K.-P. Bohnen, and K. M. Ho, Phys. Rev. Lett. **69**, 1672 (1992).

⁸S. Chiang, R. J. Wilson, Ch. Gerber, and V. M. Hallmark, J. Vac. Sci. Technol. A **6**, 386 (1988).

⁹G. W. Graham, Surf. Sci. **184**, 137 (1987).

¹⁰K. M. Ho and K. P. Bohnen, Phys. Rev. Lett. **59**, 1833 (1987); C. L. Fu and K. M. Ho, Phys. Rev. Lett. **63**, 1617 (1989).

¹¹E. S. Hirschorn, T. Miller, M. Sieger, and T.-C. Chiang, Surf. Sci. **295**, L1045 (1993).

¹²J. F. Van der Veen Surf. Sci. Rep. **5**, 199 (1985).

¹³J. K. Gimzewski, R. Berndt, and R. R. Schlittler, Surf. Sci. **247**, 327 (1991); Phys. Rev. B **45**, 6844 (1992).

¹⁴S. Chiang and S. Rousset (unpublished).